

## 3-2 Hologram Generation Technique Using Integral Photography Method

OI Ryutaro, SENOH Takanori, YAMAMOTO Kenji, and KURITA Taiichiro

When a hologram is generated using a real photographic space as its object, one must basically record the interference between beams reflected through a coherent beam illuminated on the subject on one hand, and a reference beam on the other. This method essentially requires photography in a darkroom, however, and faces many other constraints when considering its use in ultra-realistic communication. In the field of optical holography, on the other hand, the holocoder-hologram method where the first exposure is used to take integral images of the subject through many lenses and a second exposure is used to generate a hologram based on integral images is already known. The use of this two-step photography in generating electronic holograms is expected to enable the generation of holograms as electronic data of subjects taken under natural light beams, thereby expanding the applicable scope of holography. In transforming holocoder-holograms into electronic form, the coauthors have proposed a method that entails positioning hologram generation on the rear focus plane of the integral lens array, thereby transforming 3D image information recorded on integral images through a single Fourier transform operation into a complex amplitude distribution of the object beam on the hologram plane. This method makes it possible to perform transformation operation on all elemental images constituting the integral image independently of each other, and also enables fast transformation of high-resolution integral images based on many lenses through parallel calculation. Experiments conducted by the coauthors used integral images of  $4096 \times 2048$  pixels generated by computer graphics as inputs, and demonstrated that 3D images of a subject can be reconstructed from holograms generated by using the proposed method. This paper presents the details of this method.

### *Keywords*

Hologram, Integral photography, Computer-generated hologram, Real scene, Real-time

### 1 Introduction

Holographic technology is a display method that accurately records and reproduces the wave front of light emitted by a body, and which satisfies binocular parallax, kinetic parallax, accommodation, and all other clues through which humans sense the stereoscopic nature of an object<sup>[1]</sup>. For that reason, it is considered an ideal method of recording and reproducing 3D images. However, a hologram requires the recording and reconstruction of

interference fringes as fine as its wavelength. The difficulty of such operations currently limits its practical use in photographic film and other limited fields that use special metal foils with pictures drawn by means of electron beams. If it becomes possible to perform all the processes (recording, transmission and reconstruction) of real-scene holograms in an electronic and easy manner, then hopes run high that this will bring about great advances in the field of ultra-realistic communication. In particular, this paper proposes the technology for

recording real-scene holograms electronically. It is known that integral photography—whereby pictures are taken of a subject through a lens plate consisting of many convex lenses—enables 3D information of the subject including its horizontal and vertical parallax to be recorded[2]. The coauthors have observed that it is possible to generate holograms (interference fringes) as electronic data by obtaining the complex amplitude of the object beam on the hologram plane by performing Fourier transform on each element independently, after adding an appropriate initial phase to data obtained by means of this integral photography[3]. The following describes this method.

## 2 3D recording method for subject images

### 2.1 Holographic recording

The generation of real-scene holograms requires that interference fringes between the coherent beam and reference beam reflected from the subject should be photographed regardless of whether employing a photographic technology or technology based on CCD/CMOS or other electronic image sensor. Therefore, pictures of holograms had to be taken in a specialized darkroom environment with extremely low vibration.

When one uses computer graphics (CG)—where the structure of the subject is known—as the original pictures, however, the desired holograms can be generated by creating the coherent object beam reflected from the CG object in a computer and calculating the complex sum of that beam with the reference beam similarly obtained through calculation. This method is already known as the computer-generated hologram (CGH)[4]. If it were hypothetically easy to obtain a complete structural model and the texture of real-scene objects and scenes in an easy real-time manner, the CGH method could be used to generate holograms. However, under present conditions it is very difficult to obtain a detailed and faithful real-scene structural model and texture applicable to holograms.

Taking pictures of a subject from numerous viewpoints, on the other hand, is known to provide 3D information including horizontal parallax, vertical parallax, and the imaging of object points constituting the subject or scene. This is called integral photography[2]. Moreover, the holocoder-hologram has also been proposed in the past as an optical technology[5]. This technology uses images taken from many viewpoints as the original, thereby obtaining holograms of the subject optically. This method utilizes still integral images and the hologram's recording plane to prepare holograms of still real-scene images taken under a natural beam. But since this preparation of holograms requires an optical system including many lenses of very high precision, the method was not put to practical use. Moreover, when the integral photography is applied as an electronic medium, it is still necessary to conduct exposure in a darkroom, which limits its scope of application.

### 2.2 Recording using integral photography

Integral photography is also one of the methods used for recording and reconstructing images of a subject in a 3D manner. This is a beam reconstruction type of 3D recording technology and entails taking photos with a natural beam (incoherent beam) applied to the subject, as is similarly done in ordinary TV photography.

Since outdoor photography is affected by sunlight, photography by means of an incoherent beam is an indispensable requirement. Figure 1 shows the principles of recording and reconstructing 3D images by using integral photography. When taking pictures, the subject is recorded through a lens array composed of many convex lenses (elemental lenses) as shown in Fig. 1 (a). At that time, the recording plane receives many miniscule images (elemental images) obtained by observing the subject from different angles. The recording plane is positioned at the focal point distance of each lens, so that the pixels constituting the elemental images will match the direction of the paral-

lens beam that passed through the corresponding elemental lens. Similarly, the light emitted from one point on the subject plane is sampled in the same number as that of elemental lenses constituting the lens array. That is, one can see that the number of elemental lenses corresponds to the number of beams recorded.

Next, as shown in Fig. 1 (b), after the elemental image is reversed at recording, the natural beam (incoherent beam) is applied similarly from the direction where the subject was present at the time of photography. Then, passing an image through the lens eye of the same array as at the time of photography causes the beam emitted by the elemental image to be refracted by the lens array, resulting in the reconstruction of a beam equivalent to that emitted from the subject at the time of recording.

Integral photography makes it possible to

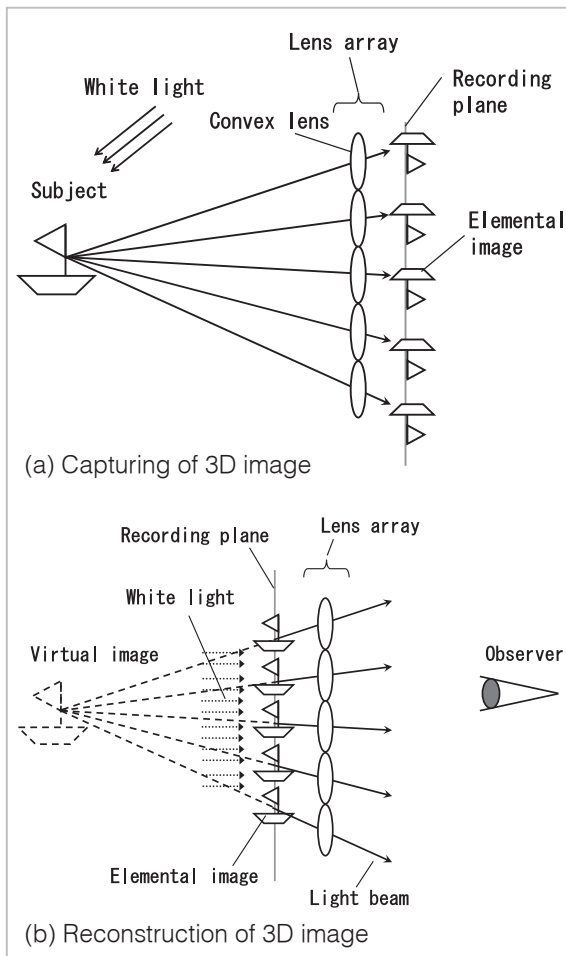


**Fig.1** Recording and reconstruction by integral photography

reconstruct the horizontal and vertical parallax, and imaging position of the subject. However, the width of reconstructed beams cannot be less than the diameter of convex lenses constituting the lens array. For that reason, the subject image to be reconstructed will have blurs as large as the diameter of lenses constituting the lens array[6].

### 3 Generation of holograms using integral photography

#### 3.1 Conversion from integral photography

When a hologram is prepared from an integrally photographed recording plane, a coherent beam is first applied to illuminate the recording plane as shown in Fig. 2, thereby reconstructing the coherent object beam. Moreover, when a reference beam that can interfere with the one used in illumination is irradiated on the hologram plane, the square of the absolute value of the complex sum of the coherent object beam and reference beam is recorded on the hologram's recording plane as an amplitude hologram. A hologram recorded this way can be used to reconstruct the original 3D image of the subject[5].

Conducting this process optically required a lens array with high positional precision and an exposure process for holograms based on a coherent beam (laser). Replacing the hologram generation process with calculation operations enables the creation of holograms without

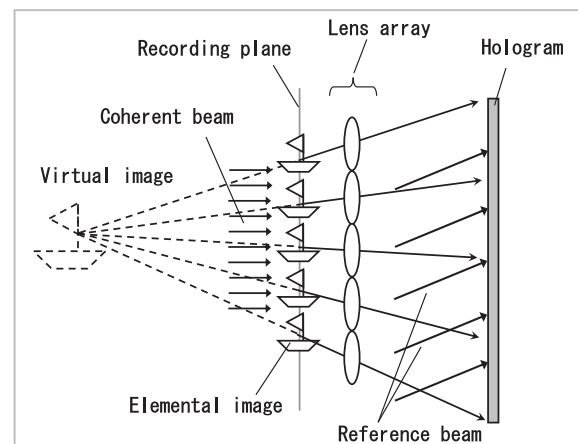


**Fig.2** Recording by holocoder-hologram

needing a darkroom for exposure[7].

When replacing the process for optically preparing holograms with CGH, people generally use a method that involves tracing the propagation of object beams by approximation in the Fresnel region of the Kirchoff diffraction integration equation.

Here, assuming an aperture and screen as shown in Fig. 3, when a wave having a complex amplitude of  $\Psi(x, y)$  passes the opening and illuminates a screen at distance  $z$ , then the complex amplitude distribution  $\Psi'(x', y')$  produced on the screen is expressed by the following equations:

$$\Psi'(x', y') = \iint_{-\infty}^{\infty} f(x, y) \cdot \Psi(x, y) \cdot \frac{1}{j\lambda r} \cdot e^{-jkr} dx dy \quad (1)$$

$$r = \sqrt{(x' - x)^2 + (y' - y)^2 + z^2} \quad (2)$$

$$k = \frac{2\pi}{\lambda} \quad (3)$$

Here, the aperture function  $f(x', y')$  is based on an aperture of 1 and a masking of 0 with  $\lambda$  as the wavelength of the light source.

Developing  $r$  to the primary term in relation to  $z$  will produce an equation as shown below.

$$r \approx z + \frac{(x' - x)^2 + (y' - y)^2}{2z} \quad (4)$$

Moreover, when the tertiary term is sufficiently small relative to the wavelength and is:

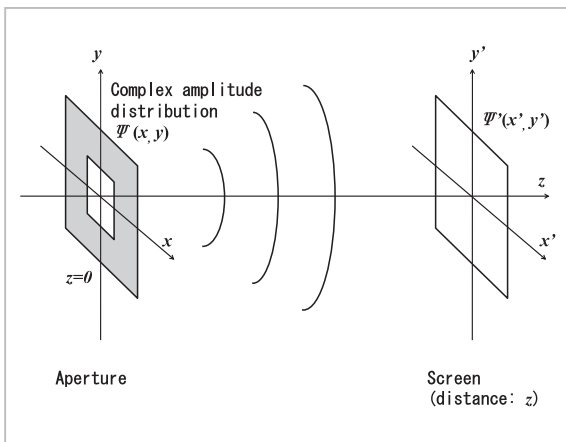


**Fig.3** Diffraction and propagation of beams in the Fresnel region

$$\lambda \gg \frac{\{(x' - x)^2 + (y' - y)^2\}^2}{8z^3} \quad (5)$$

Then the approximation of Equation (4) holds and the following equation is obtained.

$$u(x', y') = \frac{1}{j\lambda z} e^{-jkz} \iint_{-\infty}^{\infty} g(x, y) \cdot e^{-jk \frac{(x' - x)^2 + (y' - y)^2}{2z}} dx dy \quad (6)$$

Here,  $g(x, y)$  denotes the complex amplitude distribution (transformed data) in the opening;  $u(x', y')$  denotes the complex amplitude distribution (transforming data) produced on the screen.

Figure 4 shows the hologram preparation process using integral photography. First, assuming a complex amplitude of  $g_0(x_0, y_0)$  for the elemental image, one should determine the beam distribution  $g_1(x_1, y_1)$  formed on the incidence plane of the convex lens when this propagates over focal point distance  $f$  of the lens array. This can be expressed by Equation (6) as follows:

$$g_1(x_1, y_1) = \frac{1}{j\lambda z} e^{-jkf} \iint_{-\infty}^{\infty} g_0(x_0, y_0) \cdot e^{-jk \frac{(x_1 - x_0)^2 + (y_1 - y_0)^2}{2f}} dx_0 dy_0 \quad (7)$$

Next, one should determine the beam distribution  $g_2(x_1, y_1)$  formed on the exit plane of the convex lens. The resulting amplitude will remain unchanged relative to the beam distribution on the incidence plane of the lens, with

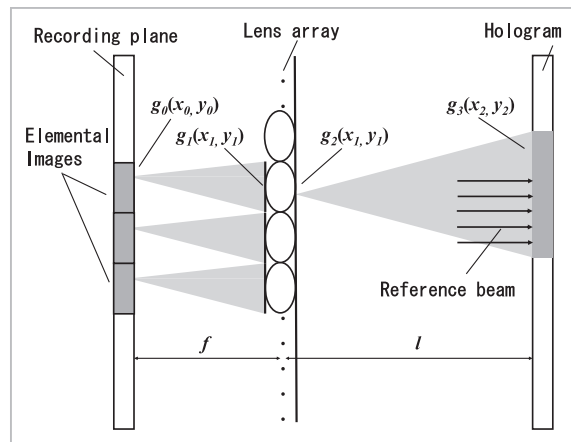


**Fig.4** Generation of holograms based on integral images

only the phase being changed and resulting in the following:

$$g_2(x_1, y_1) = g_1(x_1, y_1) \cdot e^{\frac{jk(x_1^2 + y_1^2)}{2f}} \quad (8)$$

The calculations performed so far can be determined independently for each elemental image. Furthermore, one should also determine the beam distribution  $g_3(y_2, y_2)$  on the hologram plane placed at distance  $l$  from the lens array. Again by using Equation (6), this becomes as follows:

$$g_3(x_2, y_2) = \frac{1}{j\lambda z} e^{-jkl} \int_{-\infty}^{\infty} \int_{-\infty}^{\infty} g_2(x_1, y_1) \cdot e^{-jk \frac{(x_2 - x_1)^2 + (y_2 - y_1)^2}{2l}} dx_1 dy_1 \quad (9)$$

Note that the calculations in Equation (9) must absolutely be performed on the entire hologram plane, and not just for each elemental image.

Last but not least, determining the square of the absolute value of the sum (complex sum) of the complex amplitude distribution obtained from Equation (9) and the reference beam will produce an amplitude hologram.

Here, it is notable that distance  $l$  between the hologram location and the lens array is as desired, and that the location for hologram preparation may be either immediately behind or far from the lens array.

In concrete calculations, Equations (7) and (9) must be calculated at least twice, dominated by the amount of calculations for this Fresnel transform. Conversely, the amount of calculations for Equation (8)—the modulation of the phase component from the convex lens—is comparably and negligibly small.

For efficient calculation of the Fresnel transform as shown in Equation (6), there is a solution method<sup>[8]</sup> that transforms this into a combination of Fourier transforms and then applies FFT. Here, by ignoring the constant term  $\frac{1}{j\lambda z} \exp(-jkz)$  and using a convolution integral to write Equation (6), we have the following:

$$u(x', y') = g(x, y) * p(x, y) \quad (10)$$

Here, transfer function  $p(x, y)$  is:

$$p(x, y) = e^{-jk \frac{x^2 + y^2}{2z}} \quad (11)$$

Let the Fourier transforms of  $u(x', y')$ ,  $g(x, y)$  and  $p(x, y)$  be  $U(\xi, \eta)$ ,  $G(\xi, \eta)$  and  $P(\xi, \eta)$ , respectively, and we obtain the following:

$$U(\xi, \eta) = G(\xi, \eta) \cdot P(\xi, \eta) \quad (12)$$

Then determining the Fourier transforms of  $g(x, y)$  and  $p(x, y)$ , and performing a reverse Fourier transform on the product thereof will produce  $u(x', y')$ . The Fourier transform of the transfer function can be analytically determined and will be as follows:

$$P(\xi, \eta) = e^{j\pi\lambda z(\xi^2 + \eta^2)} \quad (13)$$

Therefore, Equation (9), which is the Fresnel transform, can actually be calculated by multiplying the Fourier transform of  $g_2(x_1, y_1)$  by  $P(\xi, \eta)$  and performing a reverse Fourier transform on the result (two FFTs). With this calculation method, transformed data  $g_3(x_2, y_2)$  can be obtained with the same sampling interval and aperture width as those of transformed data  $g_2(x_1, y_1)$ .

In the hologram generation process using integral photography, Fresnel transform of the same size as the hologram plane must be used in calculations of object beam propagation from the exit plane of the lens array to the hologram plane shown in Fig. 4. Hypothetically, if fast operations are used based on FFT, performing those calculations will ultimately take much time.

### 3.2 Conversion method with easy parallel calculation

When holograms are prepared in a special location in the hologram preparation process using integral photography, transformation can then be performed more efficiently without affecting the image quality. As shown in Fig. 5, let the complex amplitude distribution formed by a single elemental image on the hologram plane be  $g_4(x_3, y_3)$ . Moreover, let the hologram plane be near the rear focal plane at distance  $d$  from the lens exit end, and use function  $h$  de-

defined by the equation below to notate the phase term as follows:

$$h(x, y; d) \equiv e^{-jk \frac{x^2 + y^2}{2d}} \quad (14)$$

As such, the optical field produced on the hologram plane by complex amplitude distribution immediately after the lens can be written by modifying Equation (6) as follows:

$$g_4(x_3, y_3) = \frac{e^{-jk d}}{j\lambda d} \cdot h(x_3, y_3; d) \cdot \iint_{-\infty}^{\infty} g_2(x_1, y_1) \cdot h(x_1, y_1; d) \cdot e^{jk \frac{x_1 x_3 + y_1 y_3}{d}} dx_1 dy_1 \quad (15)$$

Then by performing the Fresnel transform from the elemental image to the incidence end of the lens, and substituting Equations (7) and (8) that express phase modulation by the lens, the optical field produced by a single elemental image on the hologram plane can be written as follows:

$$g_4(x_3, y_3) = \frac{e^{-jk(f+d)}}{\lambda^2 f d} \cdot h(x_3, y_3; d) \times \iint_{-\infty}^{\infty} g_0(x_0, y_0) \cdot h(x_0, y_0; f) \cdot \iint_{-\infty}^{\infty} h(x_1, y_1; d) \cdot e^{j2\pi \left[ x_1 \left( \frac{x_0 + x_3}{\lambda f} + \frac{x_3}{\lambda d} \right) + y_1 \left( \frac{y_0 + y_3}{\lambda f} + \frac{y_3}{\lambda d} \right) \right]} dx_1 dy_1 dx_0 dy_0 \quad (16)$$

Here, the Fourier transform of  $h(x_1, y_1; d)$  will become:

$$\exp \left\{ j\pi \lambda d \left[ \left( \frac{x_0}{\lambda f} + \frac{x_3}{\lambda d} \right)^2 + \left( \frac{y_0}{\lambda f} + \frac{y_3}{\lambda d} \right)^2 \right] \right\} = h \left( \left( \frac{x_0}{\lambda f} + \frac{x_3}{\lambda d} \right) \left( \frac{y_0}{\lambda f} + \frac{y_3}{\lambda d} \right) \frac{-1}{\lambda^2 d} \right) \quad (17)$$

due to its relations with Equation (13). Therefore, by substituting Equation (17) in Equation (16) and omitting the constant terms, we obtain the following:

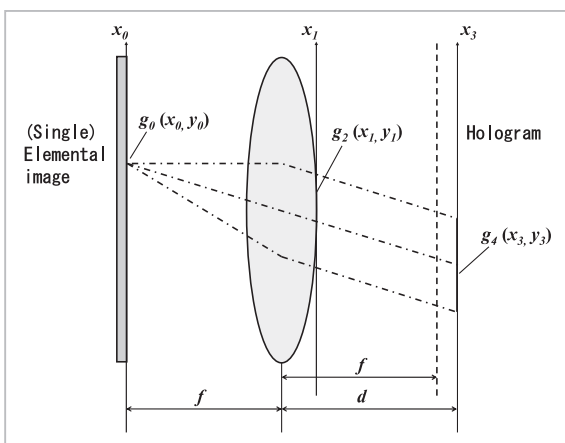


**Fig.5** Beam distribution before and after the rear focal plane of the lens

tain the following:

$$g_4(x_3, y_3) = h(x_3, y_3; d) \cdot \iint_{-\infty}^{\infty} g_0(x_0, y_0) \cdot h(x_0, y_0; f) \cdot h \left( \left( \frac{x_0}{\lambda f} + \frac{x_3}{\lambda d} \right) \left( \frac{y_0}{\lambda f} + \frac{y_3}{\lambda d} \right) \frac{-1}{\lambda^2 d} \right) dx_0 dy_0 \quad (18)$$

The terms including  $(x_3^2 + y_3^2)$  also delete each other, thereby obtaining the following:

$$g_4(x_3, y_3) = \iint_{-\infty}^{\infty} g_0(x_0, y_0) \cdot e^{-j \frac{k}{2f} (x_0^2 + y_0^2) \left( 1 - \frac{d}{f} \right)} \cdot e^{jk \frac{x_0 x_3 + y_0 y_3}{f}} dx_0 dy_0 \quad (19)$$

Here, Equation (19) is such that, when the hologram plane is  $d = f$  on the focal plane, the terms including  $(x_0^2 + y_0^2)$  in the integration can also be deleted, so that a complete Fourier transform [9] will be formed on the rear focal plane, including the phase terms of beam distribution on the front focal plane with the elemental image in place. Since this complex amplitude distribution is the object beam to be determined, when the hologram plane is the rear focal plane, the complex amplitude on the hologram plane of beam propagation before and after the convex lens can be directly determined by performing Fourier transform on the complex amplitude of the elemental image for each element, instead of performing operations based on Equations (7), (8), and (9).

Figure 6 shows the proposed method of generating holograms. Assuming that the lens array is composed of convex lenses with focal point distance  $f$ , the beam distribution on hologram plane  $g_4(x_3, y_3)$  when using the method shown in Fig. 6 will eventually be obtained with the following equation by using Equation (19).

$$g_4(x_3, y_3) = \int_{-\infty}^{\infty} \int_{-\infty}^{\infty} g_0(x_0, y_0) \cdot e^{j2\pi \frac{x_0 x_3 + y_0 y_3}{\lambda f}} dx_0 dy_0 \quad (20)$$

An amplitude hologram is obtained from the square of the absolute value of the sum (complex sum) of the finally obtained beam distribution  $g_4(x_3, y_3)$  and the reference beam.

In Equation (20), FFT operation can be used as Fourier transform. When compared with the case where holograms are prepared at a desired location at distance  $l$  from the lens array, operations can be performed more effi-

ciently. Moreover, at that time, if the beam distribution  $g_4(x_3, y_3)$  formed on the hologram plane is obtained at the same sampling distance and aperture width as those of source elemental image  $g_0(x_0, y_0)$ , then the object beams produced by element images on the hologram plane will not overlap, but appear in a manner that covers the entire hologram without gaps. This means that operations on the object beams on the hologram plane can be performed completely independently for each elemental image, and that parallel calculations can be performed on computers of the distributed memory type. When parallel operations are performed, operation units can be divided to the number of elemental images (equal to the number of lenses) at the maximum, which can realize high speed mounting.

Note that limiting the location for preparing holograms to the rear focal plane of the integral lens will do nothing but fix the relative positional relationship between integrally photographed elemental images and holograms. In ordinary integral photography, pictures are taken of a subject positioned at a desired location a certain distance away from the lens array, so that images of the subject as reconfigured from a hologram generated by the abovementioned transformation method can be produced naturally in a 3D manner at a desired location from the hologram plane. In other words, when this is regarded as a function of recording and reconstructing 3D images, there are no special constraints due to the proposed method of ho-

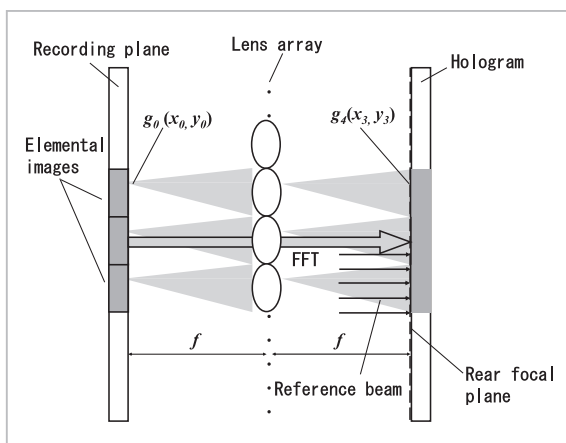


**Fig.6** Method of generating holograms with easy parallel calculation

logram generation.

### 3.3 Initial phase

Elemental images taken using integral photography technology record the amplitude of a beam alone and do not record phase information in a strict sense. For that reason, an appropriate initial phase must be given to obtain the complex amplitude distribution  $g_0(x_0, y_0)$  of elemental images in transformation Equation (20). In CGH, random phase [10] is often superimposed, assuming that the subject surface follows the Lambert reflection model. The initial phase of integrally taken elemental images is similarly set to a random phase. Therefore, the complex amplitude distribution  $g_0(x_0, y_0)$  of object beams on the surfaces of elemental images is expressed by using the luminance distribution  $A(x_0, y_0)$  of integrally taken elemental images as follows:

$$g_0(x_0, y_0) = A(x_0, y_0) \cdot e^{j \cdot 2\pi \cdot rnd(x_0, y_0)} \quad (21)$$

In Equation (21), note that  $rnd(x_0, y_0)$  is a uniform random number in the interval [0,1).

### 3.4 Color 3D image

The discussion above regarded a case using a coherent beam with single wavelength  $\lambda$ . In holographic technology, the basic principle is to record 3D images of a subject by using a single wavelength. However, recording holograms with the three colors (red, green and blue) of coherent beams as in TV broadcasting, and also illuminating with coherent beams of the same wavelength at reconstruction will enable the reconfiguration of 3D color holographic images.

In the proposed method, the same applies to generating holograms from integrally taken original pictures. Coherent beams near the central wavelength of RGB filters in a color camera at the time of integral photography can be used to transform images into holograms corresponding to the three primary colors, in order to prepare color holograms.

## 4 Optimal design of elemental images as the result of discretization

When FFT or other discrete numerical calculation is used in generating holograms from integrally taken original pictures, the focal point distance of the integral lens, the number of samples of elemental images, and various other design values must be determined to ensure proper mounting.

With the algorithm of the commonly used discrete Fourier transform, let the transformed function be set to  $g(m, n)$  and the Fourier spectrum on Fourier transform plane  $j-k$  be  $G(j, k)$ , with their relationship being expressed by the following equation:

$$G(j, k) = \sum_{m=1}^M \sum_{n=1}^N g(m, n) \cdot e^{j2\pi(\frac{jm}{M} + \frac{kn}{N})} \quad (22)$$

The following equation is conversely the result of rewriting Equation (20) to determine the beam distribution on the hologram plane from integrally taken elemental images with the numbers of horizontal and vertical samples set to  $M$  and  $N$ , respectively, and the sampling interval set to  $\Delta p$ , in order to Fourier-transform it as data discretely sampled in a limited aperture.

$$g_4(x_5\Delta p, y_5\Delta p) = \sum_{x_4=1}^M \sum_{y_4=1}^N g_0(x_4\Delta p, y_4\Delta p) \cdot e^{j2\pi \frac{x_5x_4 + y_5y_4}{\lambda f} \Delta p^2} \quad (23)$$

Here, let the conditions be that the elemental image, size (aperture), and sampling interval of the element hologram calculated from the elemental images and this elemental image are equal, and that the element holograms do not overlap but are laid throughout without gaps, thereby obtaining the following relational equations from a comparison of the phase terminals in Equations (22) and (23).

$$M \cdot \Delta p^2 = \lambda \cdot f \quad (24)$$

$$N \cdot \Delta p^2 = \lambda \cdot f \quad (25)$$

From this, one can see that focal point distance  $f$  in calculations of the process for generating holograms from original pictures recorded in integral photography is determined by sam-

pling interval  $\Delta p$  of the original picture, calculation wavelength  $\lambda$ , and the number of samples ( $M$  or  $N$ ).

For simplification, the following discussion will be based on the assumption that the horizontal and vertical sampling intervals are equal ( $M = N$ ), and that the aperture widths are also equal, being rectangular ( $N\Delta p$ ).

When one thinks of determining the distribution of complex amplitudes of object beams on the hologram plane by using FFT in Equation (20), one can choose  $N$  as two's power to perform efficient transformation. As an example, when using a value from Table 1 as a parameter to generate a hologram from an integral image, one can see from the relationship in Equation (25) that focal point distance  $f$  of the integral lens in the calculation is 0.582 mm.

In integral photography, it is known that the ratio of the lens diameter in photography to the lens diameter in reconstruction will be the lateral magnification of the image to be reconstructed (i.e., magnification of the image height), and that the ratio of the lens focal point distance in photography to the focal point distance in reconstruction will become the longitude magnification in reconstruction (i.e., magnification of depth). Therefore, if, hypothetically, the focal point distance of the elemental lens in integral imaging as shown in Fig. 7 is 12 mm, then the optimal design lens pitch (diameter) in photography will be 1.583 mm, and the reconstructed holographic image at that time will be strain-free as a 3D image. Moreover, in that case, the view angle that allows for the subject by integral imaging will be about 7.54 degrees.

## 5 Generation and reconstruction of holograms by computer simulation

Computer simulation was conducted to generate holograms based on the proposed method from integrally taken original pictures.

### 5.1 Preparation of integral images

Here, in preparation for the original pic-

tures, CG pictures that simulate the subject with a two-layer depth as shown in the layout in Fig. 8 were used to prepare integral images of 4096 pixels horizontally by 2048 pixels vertically. Table 2 lists the parameters used in preparing integral images. Here, the focal point distance and aperture of the lens were set to 10 times their respective settings listed in Table 1. Figure 9 shows the original pictures prepared. One can see that the original pictures have the arrangement structure of the elemental lens. Moreover, one can also see changes in the image of the subject appearing in the elemental image according to the distance of the subject.

## 5.2 Hologram generation

Next, the algorithm shown in Fig. 10 was followed to transform the data into hologram data. First, a random phase of 0 to  $2\pi$  was given to the elemental image composed in units of 16

**Table 1** Examples of settings made in hologram generation

Sampling interval : $\Delta p$	4.8 $\mu$ m
Number of horizontal and vertical samples : $N$	16
Calculated wavelength : $\lambda$ (He-Ne red)	633nm
Lens aperture diameter : $N\Delta p$	0.0768mm
Lens focal point distance in calculation : $f$	0.582mm

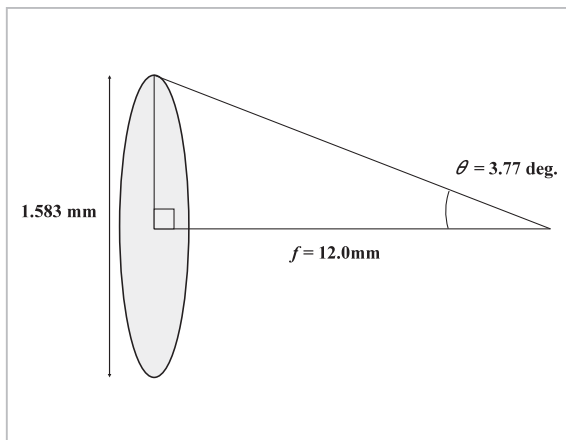


**Fig.7** Examples of settings made on the elemental lens in integral imaging

$\times 16$  pixels, and then two-dimensional FFT was performed based on the DC component as the image center. The data obtained was the distribution of complex amplitudes of object beams in the hologram's recording plane, as determined independently of the elemental images. Calculations were also performed on the interference fringes between the object beam obtained and the reference beam. Here, it was assumed that the reference beam was to enter from the direction vertical to the hologram. The reference beam  $R_{(y)}$  used in calculations for the off-axis hologram that enters at angle  $\theta$  can be given by the equation below. Here,  $k$  denotes the wave number ( $k = 2\pi/\lambda$ ).

$$R_{(y)} = |R| \cdot e^{jk \cdot \sin \theta \cdot y} \quad (26)$$

The beam that enters a hologram vertically becomes a reference beam having constant ampli-

**Table 2** Parameters used in recording integral images

Focal point distance of lens : $f$	5.82mm
Aperture diameter of lens : $D$	0.768mm
Elemental image size : $N$	16 horizontally $\times$ 16 vertically
Number of elemental images	256 horizontally $\times$ 128 vertically
Total number of pixels	4096 pixels horizontally $\times$ 2048 pixels vertically

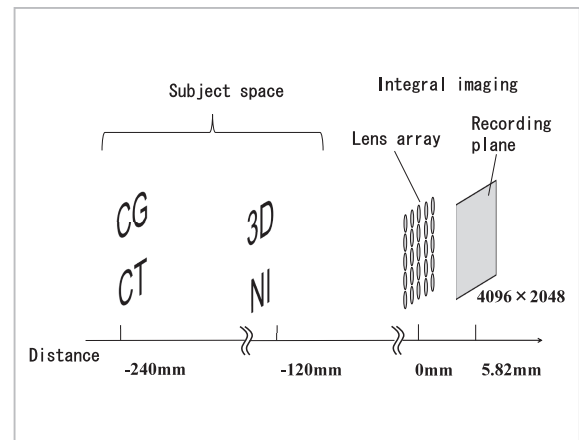


**Fig.8** Layout of the subject in recording integral images

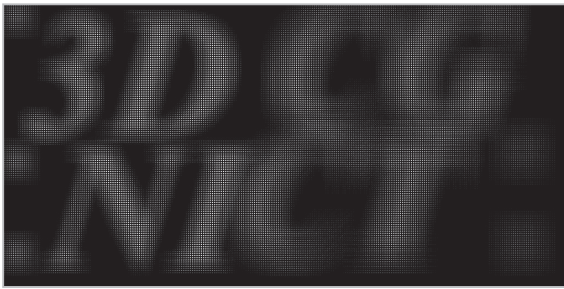


**Fig.9** Integral image (4096 × 2048 pixels) used in experiments

**Table 3** Parameters used in hologram generation

Total number of hologram pixels	4096 pixels horizontally × 2048 pixels vertically
Pixel pitch : $\Delta p$	4.8 $\mu$ m (horizontally & vertically)
Elemental hologram dimensions	16 horizontally × 16 vertically
Wavelength : $\lambda$	633nm (He-Ne red)
Focal point distance of lens : $f$	0.582mm (calculated value)
Reference beam	Parallel beam (in-line)

tude on the entire screen obtained by substituting  $\theta = 0$  in Equation (26), and after all, the hologram is nothing but the real portion of the object beam. Table 3 lists the settings used in hologram generation; Figure 11 shows the holograms obtained.

### 5.3 Hologram reconstruction

Holograms obtained using the abovementioned method were reconstructed by computational reconstruction to observe the images. Here, how imaging is performed on a plane separated by distance  $-z$  from the hologram's recording plane is reproduced. Figure 12 shows hologram images reconstructed over two different distances from the hologram plane. Figure 12 (a) shows a reconstructed image at a distance close to the hologram plane. In Fig. 8, the subject placed close to the integral recording plane is sharply imaged, and one can see here that the subject placed far from the recording plane is reconstructed as being blurred.

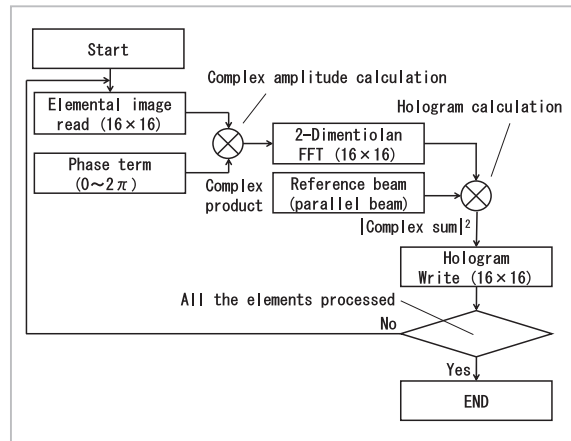


**Fig.10** Processing to generate holograms from integral images



**Fig.11** Hologram pattern generated (DC = 127)

Conversely, Fig. 12 (b) shows that the subject placed far from the recording plane is sharply imaged, but the subject placed close to the recording plane is reconstructed as being blurred. These results show that 3D composition of the subject space is correctly maintained by the proposed method of hologram generation. Here, the lens focal point distance and aperture in hologram generation are one-tenth the integral image, respectively, and one can see that the distance to the subject is reduced in response to the magnification. By comparing the subject shown in Fig. 8 with the position of the reconstructed hologram image, it was confirmed that the ratio of longitudinal magnification to transverse magnification of the subject was correctly stored as well.

## 6 Conclusion

This paper described a method of generating electronic holograms by using integral pho-



(a) Reconstructed image at distance of 12.58mm



(b) Reconstructed image at distance of 24.58mm

**Fig.12** Reconstructed image of a hologram (how imaging is performed at a constant distance from the hologram plane)

tography. One can perform Fourier transform on each element independently after adding an initial phase to data obtained by integral imag-

ing, thereby obtaining the distribution of complex amplitudes of object beams on the hologram plane, and thereby eventually generating holograms in a quick manner.

Moreover, the paper clarified the relationship between the focal point distance of the lens array best suited for using a fast Fourier transform (FFT) and the sampling interval for elemental images in the transformation process from integral images to holograms.

The experiments conducted involved generating and reconstructing holograms by means of the proposed method by using CG-generated integral images of  $4096 \times 2048$  pixels. From the observation results of the images reconstructed, the coauthors confirmed the possibility of obtaining 3D images that correctly reproduce the depth relationship of the subject space.

Hopes run high that by performing all the processes of real-scene holograms (recording, transmission and reconstruction) electronically and easily in the future, then great progress will be made in the field of ultra-realistic communication.

## References

- 1 R.Oi, M.Okui, "A Method for Displaying a Real-scene Fresnel Hologram," The Institute of Image Information and Television Engineers (ITE) Technical Report, Vol. 30, No. 43, pp. 3-6 (2006)
- 2 M. G. Lippmann, "Epreuves reversibles donnant la sensation du relief," Journal of Physics, 4 serie, VII , pp. 821-825, 1908.
- 3 R.Oi, T.Mishina, M.Okui, Y.Nojiri, and F.Okano, "A Fast Hologram Calculation Method for Real Objects," Journal of The Institute of Image Information and Television Engineers (ITE), Vol. 61, No. 2, pp. 198-203 (2007)
- 4 B. R. Brown and A. W. Lohmann, "Computer generated binary holograms," IBM Journal of Research and Development, 13, pp. 160-167, 1969.
- 5 R. V. Pole, "3-D Imagery and holograms of objects illuminated in white light," Applied Physics Letter, 10, pp. 20-22, 1967.
- 6 J. Arai, H. Hoshino, M. Okui, and F. Okano, "Effects of Focusing on the Resolution Characteristics of Integral Photography," Journal of Optical Society of America, Vol. 20, No. 6, pp. 996-1004, 2003.
- 7 T. Mishina, M. Okui, and F. Okano, "Generation of holograms using integral photography," in Three Dimensional TV Video and Display III, Proc. SPIE5599, pp. 114-122, 2004.
- 8 Y.Matsuo, K.Yamane, "Rader Holography," pp. 80-81, The Institute of Electronics and Communication Engineers of Japan (1980)
- 9 Y.Yamaguchi, "Applied Optics," pp.189-201, The Japan Society of Applied Physics, Ohmsha (1998)

---

10 A. W. Lohmann and D. P. Paris, "Binary Fraunhofer holograms generated by computer," *Applied Optics*, 6, 1739–1748, 1967.

(Accepted Sept. 9, 2010)



**OI Ryutaro, Dr. Sci.**

*Senior Researcher, 3D Spatial Image and Sound Group, Universal Media Research Center*

*Optical Wave Propagation Analysis, Holography, 3D Imaging Technology, Image Sensor*



**SENOH Takanori, Dr. Eng.**

*Expert Researcher, 3D Spatial Image and Sound Group, Universal Media Research Center*

*Electronic Holography, 3D Image Technology*



**YAMAMOTO Kenji, Dr. Eng.**

*Senior Researcher, 3D Spatial Image and Sound Group, Universal Media Research Center*

*Electronic Holography, 3D Image Technology*



**KURITA Taiichiro, Dr. Eng.**

*Group Leader, 3D Spatial Image and Sound Group, Universal Media Research Center*

*Television System, Information Display, 3D Image Technology*